Measurements and simulation of the dynamic responses of a bridge-embankment transition zone below a heavy haul railway line

Jin, Shi; Burrow, M. P.; Chan, Andrew; Wang, Y. J.

DOI:
10.1177/0954409712460979

Document Version
Peer reviewed version

Citation for published version (Harvard):
Jin, S, Burrow, MP, Chan, A & Wang, YJ 2013, 'Measurements and simulation of the dynamic responses of a bridge-embankment transition zone below a heavy haul railway line', *Proceedings of the Institution of Mechanical Engineers Part F Journal of Rail and Rapid Transit*, vol. 227, no. 3, pp. 254-268. https://doi.org/10.1177/0954409712460979

Measurements and simulation of the dynamic responses of a bridge-subgrade transition zone below a heavy haul railway line

Jin Shi[a], M.P.N.Burrow[b,c] , A.H. Chan[b,c], Ying Jie Wang[a,d]

[a]School of Civil Engineering, Beijing Jiaotong Unerversity, Beijing, China

[b]Centre for Railway Research and Education, University of Birmingham, Birmingham, UK

[c]School of Civil Engineering, University of Birmingham, Birmingham, UK

[d]Department of Civil and Environmental Engineering, Rutgers, The State University of New Jersey, Piscataway, New Jersey, USA

Abstract: It is an effective way to solve the current shortage of transport capacity by developing heavy haul transportation in china. However, the increasing heavy axle loads and high-density transport condition intensify the damage of track, especially in the transition zone where stiffness and deformation changed suddenly. In order to cost of maintenance, the physical mechanisms of transition zone must be investigated. Unfortunately, no further details were proposed for vibration and mechanisms of the transition zone for the heavy haul railway. In this paper, an extensive dynamic experiment was undertaken on a typical bridge-subgrade transition zone in the Shuohuang railway, China. Acceleration of the rail, sleeper and embankment in response to passenger trains were measured, many useful results have been obtained from the analysis of the recorded data. A dynamic three-dimensional finite element model was developed and validated using the measure accelerations. As a case study, dynamic response of bridge-subgrade during train passage is analyzed.

Key words: bridge-subgrade transition, field measurement, finite element, dynamic response, accelerations, embankment

1 Introduction

China is seeking to solve its current shortage of transport capacity by developing heavy haul railway. However, the associated increases in axle loads, speeds and track utilization are resulting in accelerated damage of the railway network. This is particularly evident where the structural capacity of the track has not been designed to carry these increased loads. A particular concern is so called transition zones where the stiffness of the track changes significantly over a short length. Track maintenance in such areas has been found to be up to 2-4 times greater than those on sections of track where the stiffness is continuous. This paper describes measurements of track acceleration taken at a subgrade-bridge transition on the Shuohuang railway in China and presents the development of a dynamic finite element model which can be used to investigate the design and maintenance of suitable transition zones.

Recent advances in remote condition monitoring techniques have facilitated the field measurement of railway track performance. This, together with the continuing increases in computer power which has enabled theoretical computational models of the track system to be developed, has furthered understanding of track behavior in a dynamic loading environment.

The recognition of the association of track integrity issues with abrupt changes in track stiffness has led to a great deal of recent research in this area [1~4]. A number of authors describe field measurements of the track system response in the vicinity of transition zones. For example, Coelho [5] undertook an extensive monitoring and investigation programmer in the Netherlands of a reinforced concrete approach slab transition which links the track to a concrete culvert. Accelerations and velocities of the track, soil, and the approach slabs in response to passenger trains were measured, from which displacements were calculated. Priest et al. [6] describe a detailed investigation of ground deformations that occur under a bridge-subgrade transient zone during the passage of a train on the COAL link line in south of Vryheid, South Africa. A dynamic linear-elastic two-dimensional finite element model of the transition was developed and validated using measured displacements. Others who have also developed dynamic computer models of the transition zones include Yang [7] who investigated the train induced stress regime of the track substructure by means of a two-dimensional dynamic finite-element model (FEM). The model was used to analyze the effects of train speed, acceleration and braking, geometric variation in the rail head level, and hanging sleepers. In order to investigate the influence of track stiffness on vehicle / track interactions in transition zones, Lei [8] developed a 2D dynamic FEM of the

vehicle–track–subgrade coupling system. Gallego [9] developed an FEM in order to improve transition zone design by considering the effects of variations in the geotechnical and geometrical parameters of transition zones.

For dynamic analysis such as that discussed herein, the 2D FE models described above are a significant improvement on static models as they allow the effects of train speed and the associated dynamic excitation of the track system to be taken into account in any analysis. However because of complexities associated with modeling, those described above do not incorporate accurate constitutive models of the track substructure which are necessary to properly replicate the induced stress regime in the track substructure. Further, because the models are two dimensional they are unable properly to model the effects of lateral vibration.

This paper describes an extensive research project which was undertaken on a bridge-subgrade transition zone on the Shuohuang railway, in China's Hebei province where increases in train axle loads and annual tonnage are proposed. The accelerations of the rail, sleeper and subgrade in response to the passage of freight trains were measured. To help better understand the effect of the transition zone on deterioration and the requirements for suitable strengthening measures, in light of the proposed increases in load, a three-dimensional dynamic FE model was built and validated using the measured accelerations. This is described further below.

2 Field testing

2.1 The site

The field investigation was carried out on the Shuohuang railway line. The 588 km long railway line (see Figure 1), an important route in China's coal corridor, starts from Shenchi south railway station in Shanxi province and ends at Huanghua port freight yard in Hebei province. The line carries 6.8 million tonnes of freight per year and in the next ten years this is set to increase to 100 million tonnes per year. Both the frequency of freight trains and the axle loads of wagons (from 250 kN to 300 kN) will increase.

Figure 1 Line Diagram of Shuohuang Railway

There are a large number of bridge-subgrade transition zones along the Shuohuang Railway line. Because the abrupt changes in stiffness associated with such transition zones can lead to increased track damage and pose safety issues, the aim of the research was to investigate whether such problems would become more likely should the proposed increases in train loads occur. In addition it was anticipated that the work would enable a preliminary assessment of whether the design of the existing transition zones should be modified.

To this end it was decided to analyze a short section of the Shuohuang Railway line in detail. The 200 m long section consisted of a bridge and the transition zones at either end. It was selected due to its ease of access, much of the railway passes through mountainous regions (see Figure 1). The bridge is a T girder concrete bridge 24m long (see Figure 2a). The up line is continuously welded (CWR) 75kg/m rail, with concrete sleepers at a spacing of 1.84 /m (see Figure 2b). On the down line the rail mass is 60kg/m and the sleeper arrangement is that as for the up line. A higher mass rail was used on the up line as it carries fully laden coal wagons travelling from the coal mines in Shengmu to the ship building port of Huanghua. The wagons return empty on the down line. The track substructure comprises ballast and subballast layers as shown in Figure 3. The ballast layer is approximately is approximately 0.6m deep. The subgrade comprises three distinct layers: graded broken stone of approximately 0.7 m deep, 2.3 m of clay, and a sand and gravel layer of 3.0 m.

Comment [b1]: Is this natural or engineered?

(a) T girder concrete bridge

(b) embankment

Figure 2 Transition zone of Shuohuang Railway

2.2 Test arrangement

The main focus of the research reported here was to assess the potential impact of the increased magnitude and frequency of loads on the embankment substructure track deterioration. Therefore as the dynamic loads on the substructure are greatest when the train travels from the stiffer structure to the lower stiffness substructure [5] only the embankment of the track carrying the fully laden wagons was instrumented.

Accelerations were measured using 24 accelerometers placed at six horizontal distances along the track and at four different depths as shown in Figures 3a and b. .

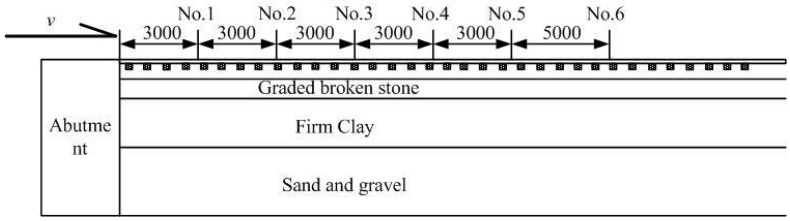

(a) The vertical section

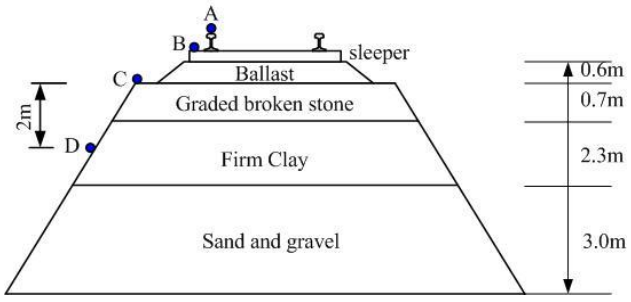

(b) The cross section

Figure 3 Sections through embankment showing locations of accelerometers

A data acquisition system of IOTECH WB-618 data loggers [10] and acceleration transducers were installed to record the measured accelerations.

2.3 Traffic loads

The freight trains using the railway line investigated typically consists of one locomotive hauling up to 66 wagons traveling at speeds of between 65 and 75 km/h. The locomotives are approximately 27 m in length with 8 axles each carrying a load of 230 kN (see Figure 4). The wagons are approximately 12 m in length and consist of four axles with loads of 250 kN. The total length of a train is approximately 850m.

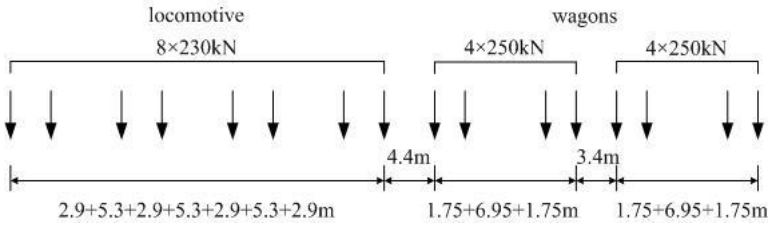

Figure 4 Composition of constant axle loads

3 Analysis of results

3.1 Frequency domain analysis

Figure 5 shows the acceleration spectrum in the frequency domain of the rail and the substructure caused by a freight train traveling at a speed of 71 km/h. It was recorded at a distance of 3 m from the abutment (see Figure 5a). From Figure 5a it may be seen that dominant frequencies of rail vibration occur at frequencies of between 500 and 1200Hz and also at between 6000 and 7000Hz. These are likely to be induced by short wavelength corrugations on the rail [11]. As far as the track substructure is concerned it is apparent from Figure 5b and Figure 5c, that at the bottom of the ballast a fundamental frequency of approximately 30-35Hz occurs. This corresponds to the sleeper spacing of 0.6 m for a freight train traveling at 71 km/h (i.e. 19.8 m/s/0.6 m = 33 Hz). An additional peak at a frequency of about 60-65Hz may also be seen and is associated with the second harmonic of the fundamental frequency associated with the sleeper intervals. The acceleration spectrum of the clay layer at 2 m depth indicates that, the high frequencies corresponding to the excitation of the rail have attenuated and that only those corresponding to the excitation of the sleepers (at about 30~35Hz and about 60~65Hz) are apparent. In addition the frequencies corresponding to individual bogies and axles can be identified, but it is unapparent. The former occur at 2.3 Hz (i.e. 19.8 m/s / 8.7 m) and the latter at 11 Hz (i.e. 19.8 m/s / 1.75 m)

Comment [b2]: Can these be identified or not?

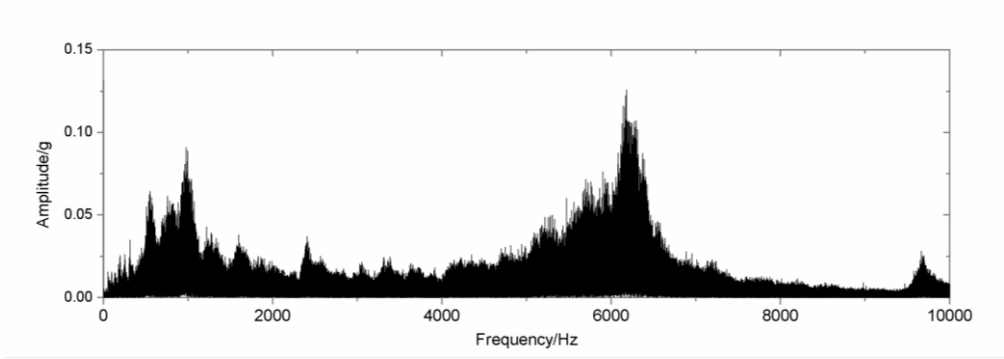

(a) Rail acceleration

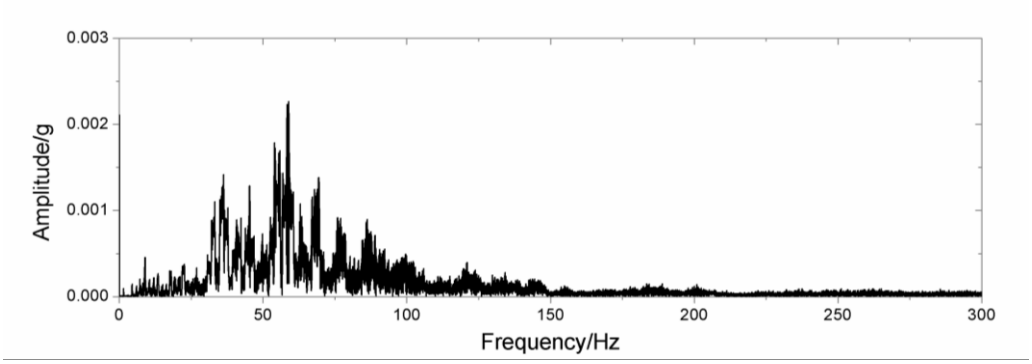

(b)Acceleration of subgrade at 0m depth

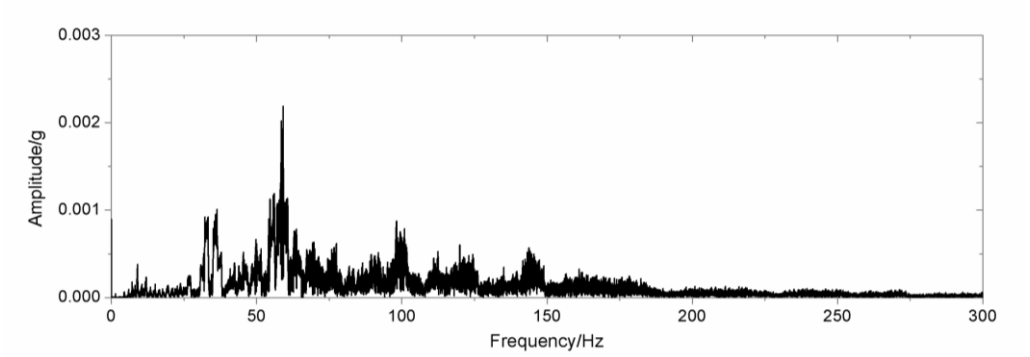

(c)Acceleration of subgrade at 2m depth

Figure 5 The acceleration spectrum for the embankment.

3.2 Time history analysis

Figure 6 shows typical accelerations of the rail and the substructure as a function of time, recorded at the location described above. From Figure 6b the accelerations due to the locomotive and the wagon train can clearly be distinguished. Those due to the locomotives occur between 2.5 and 5

seconds and are noticeably higher than those caused by the wagon train.

The peak of accelerations of the rail and substructure shown in Figure 6 correspond to individual bogies although the individual axles are not distinguishable. The peak mean measured rail acceleration was found to be in the 80 to 95g range, that of the bottom of the ballast 0.07-0.85g and between approximately 0.05 to 0.1g at a depth of 2 m.

Interestingly, whilst the individual axle loads of the locomotive are less than those of the wagons, the locomotive causes higher accelerations at the bottom of the ballast and in the clay layer. This is possibly due to the different axle configurations (Figure 4) and suggests that axle configuration is an important parameter when modeling loads and determining associated damage to the substructure. This confirms the approach of other authors who model the four axles of a wagon as a single load application in static analytical models of the track system (see for example [19]).

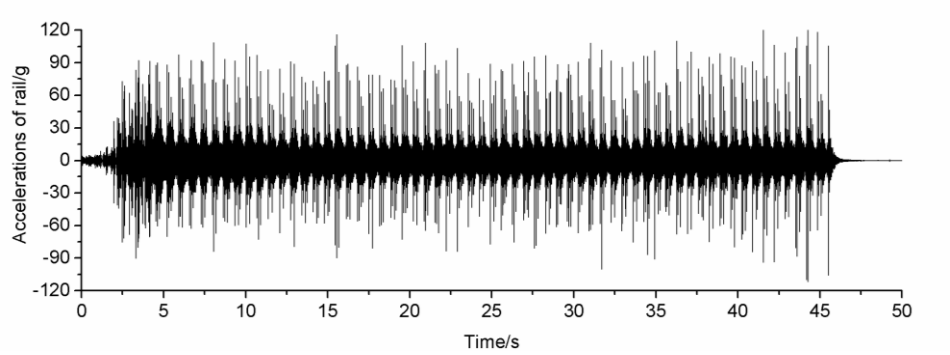

(a) Rail acceleration

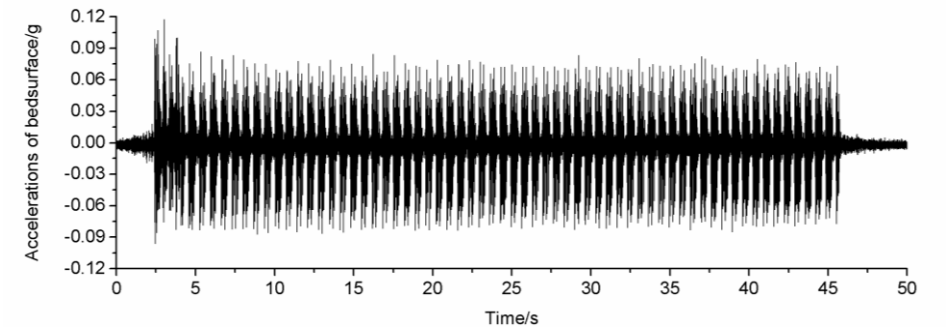

(b) Acceleration of subgrade at 0m depth

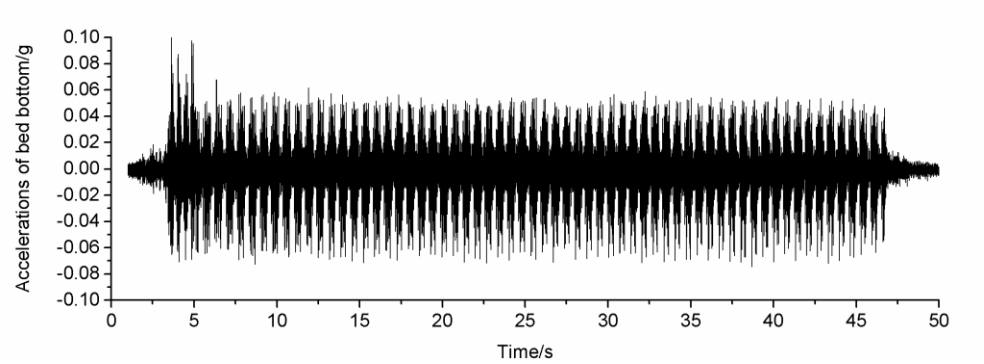

(c) Acceleration of subgrade at 2m depth

Figure 6 The accelerations at rail and embankment in 3m distant from abutment at the train speed of 71km/h

3.3 Acceleration attenuation

To analyze vibration attenuation in the transient zone, the levels of vibration were calculated using the following equation [12]:

$$VAL=20\lg\ (a_{rms}/a_0) \qquad \text{(Equation 1)}$$

Where *VAL* is the amount of vibration in dB, a_0 is reference acceleration ($a_0=1\times10^{-6}ms^{-2}$), a_{rms} is the effective value of measured acceleration in ms^{-2}, and is given by:

$$a_{rms}=\sqrt{\frac{1}{N}\sum_1^n a_n^2(t)} \qquad \text{(Equation 2)}$$

Where *t*, the running time, is the time required for the entire train to pass a particular point and *N* is the total number of measured accelerations during *t*.

a_n can be obtained from:

$$a_n=\ a'/\sqrt{2} \qquad \text{(Equation 3)}$$

Where *a*' is the measured acceleration.

Figure 7 shows the maximum acceleration along the track from which it may be seen that the vibration of the rail and sleeper are very large within 2 m of the abutment. Measured accelerations of the rail are in the order of 3 times higher than for typical values when there is no transition (i.e. 100g, compared to 30g) and for the sleepers about twice as high (10 g compared to approximately 5g). Consequently, the components in these areas are subject to very high forces and could therefore be expected to deteriorate rapidly.

It can also be seen that the vibration along the track line decays with distance from the abutment. The acceleration of the rail and the sleepers reduce by approximately 60% between 2

and 6 m away from the abutment (i.e. for the former from 100g to 40g, and for the latter from 10g to 4g). At distances greater than 6 m from the abutment the acceleration of the rail and the sleepers decay more slowly. As far as the substructure is concerned, the acceleration reduced rapidly within the embankment due to ballast and soil damping and is in the region of 0.03g-0.08g. This suggests that the deterioration of the substructure may be less influenced by the transition zone than that of the rail and sleepers. This may also suggest that the thickness of the granular layer (ballast plus subballast) is sufficient for the current axle loads (250 kN).

Figure 8 shows the levels of vibration along the track. Significant attenuation of the vibration levels occur with depth. At the rail, the amount of vibration is between 148 to 154 dB, this reduces to between 129 and 138 dB at the sleepers and then to between 95 to 100 dB in the substructure. Interestingly, the level of vibration within the embankment at a depth of 2m appears to be slightly higher than that at the bottom of the ballast.

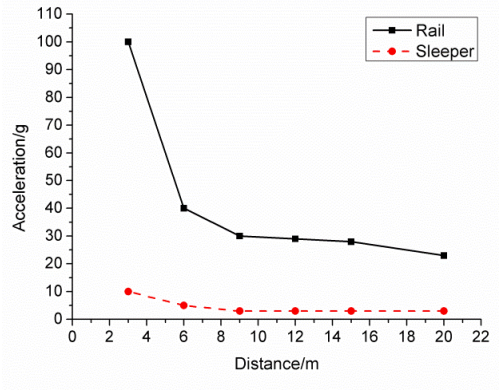

(a) Rail and sleeper

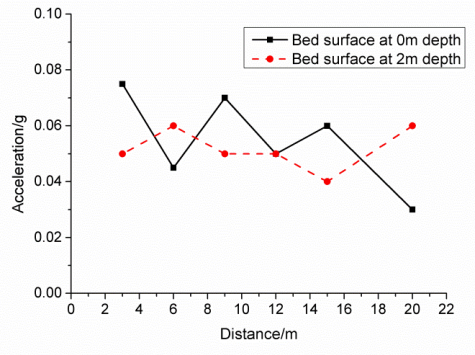

(b) Embankment

Figure 7 The maximum accelerations along the track line

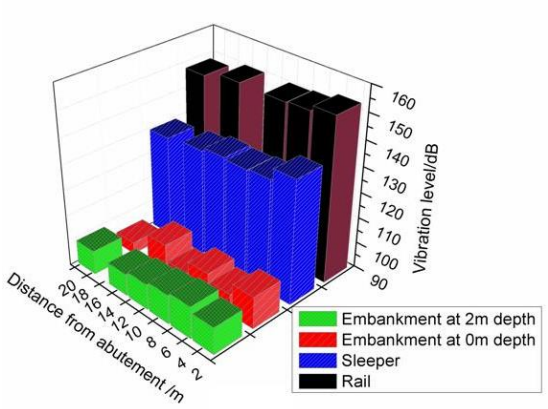

Figure 8: The vibration level along the track from the abutment

4 Development of a three-dimensional finite element model

In order to facilitate the design of appropriate transition zones which would minimize vibration of the track components and track deterioration, a 3 dimensional dynamic finite element model (FEM) of the track vehicle system was built using ABAQUS explicit software [20]. The mesh, shown in Figure 9, comprised of a total of 39998 elements and 74523 nodes making up a track length of 60m. The components of the system are described below and their associated parameters for modeling purposes are given in Tables 1 and 2.

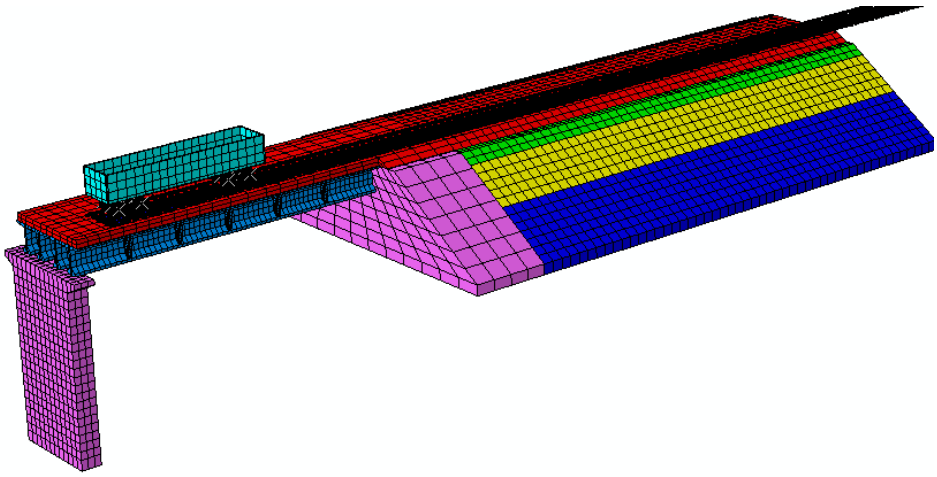

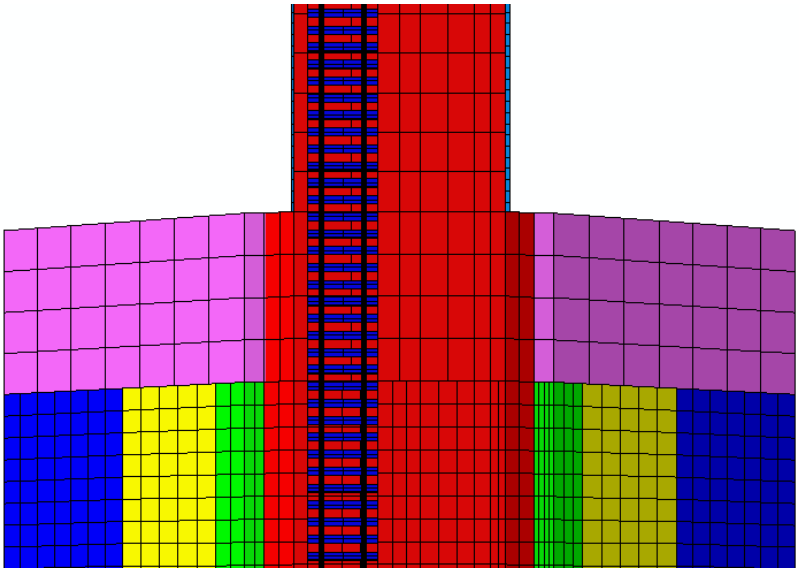

Fig.9 FE model for dynamic analysis

Comment [b3]: Figure 9:

4.1 Vehicle

The freight vehicles were idealized as a as a multi-body system consisting of a car body, bolster, frame and wheel set, with spring-dashpot suspensions between the four components as shown in Figure 10. To minimize computational time the train was modeled as a single wagon moving at 71 km/h. The associated parameters of the four components are given in Tables 1.

The following assumptions were used in modeling the train:

1. The car body bolsters frame and wheel in the vehicle were regarded as rigid components.
2. The connections between the wheel and frame, the primary suspension system, are characterized as linear springs and viscous dashpots.
3. The connections between the car-body and bolster (the secondary suspension system) are modeled as a system of linear springs and viscous dashpots in the vertical direction.
4. In the 3D model, vibration in the vertical plane only was considered.

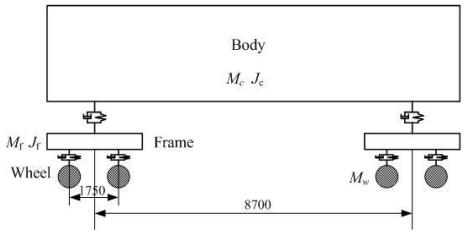

(a) The vertical section

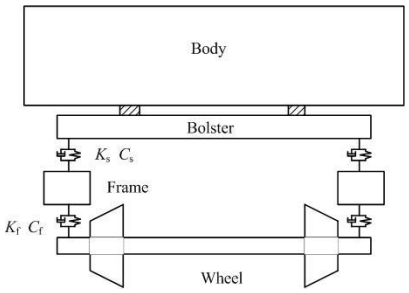

(b) The cross section

Figure 10: Idealized freight vehicle

Table 1 Freight vehicle parameters

Mass of car body *(M_c)*	91.4kg
Inertia of car body *(J_c)*	1.33×10^5 kg·m^2
Mass of frame *(M_f)*	496kg
Inertia of frame *(J_b)*	190kg·m^2
Mass of wheel *(M_f)*	1257kg
Primary suspension stiffness	13MN/m
Primary suspension damping	3×10^5 Ns/m
Secondary suspension stiffness	4.4 MN/m
Secondary suspension damping	4×10^3 Ns/m

The contact normal force between the wheel and rail was modeled as Hertzian [1]. The normal contact force P(t) can be determined using the following equation:

Comment [b4]: Check Hertzian

Comment [b5]: Check normal force

$$P(t)=\left[\frac{1}{G}\Delta Z(t)\right]^{3/}$$ (Equation 4)

Where G is the contact constant, $\Delta Z(t)$ is the elastic compression between the rail and wheel in meters.

The creep force between the wheel-rail is given by :

$$\tau_{crit} = \mu p$$ (Equation 4)

Where μ is the coefficient of friction.

The contact geometry of the wheel and rail was as shown in Figure 11.

Fig.11 Contact geometry relationship between wheel and rail

4.2 Bridge-subgrade

The track was modeled as 75kg/m steel rails at a gauge of 1435mm, supported by concrete sleepers placed at a spacing of 0.6m on a 0.6m depth of ballast. The subgrade was modeled using elastic solid elements as three layers of engineering fill, the initial Young's modulus values of which were determined using plate loading tests carried out in situ [13]. Thereafter an inverse analysis approach was used to determine the resilient modulus values of each layer to match those measured in the field. The values so determined are given in Table 2. This analysis is described in detail by [14].

Comment [b6]: What FE elements were used for the rail and for the sleepers?

The bridge model consisted of multi-span girders and piers which were modeled using 20-node quadratic brick elements. Each span was represented as a concrete T-girder, 24m in length (see Figure 12). A rectangular slab pier was used to represent the transient zone.

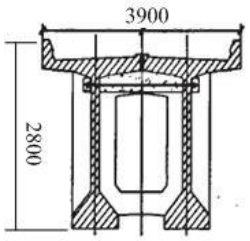

Figure 12: The cross section of a girder

Table 2 Materials properties parameters in FE model

Component	Property	Value
Rail	Young's modulus, GPa	210
	Poisson's ratio, ν	0.3

	Density kg/m^3	7830
Sleeper	Young's modulus, GPa	35
	Poisson's ratio, ν	0.22
	Density kg/m^3	2600
	Dimnesions(L,W,H),m	2.5,0.25,0.16
Fastener	Vertical stiffness,kN/mm	90
	Vertical damping kN.s/m	75
	Horizontal stiffness, kN/mm	45
	Horizontal damping ,kN.s/m	60
Ballast	Young's modulus, MPa	180
	Poisson's ratio, ν	0.27
	Density kg/m^3	1650
	Thickness,m	0.6
Graded broken stone	Young's modulus, MPa	180
	Poisson's ratio, ν	0.3
	Density kg/m^3	2300
	Thickness,m	0.7
Clay	Young's modulus, MPa	130
	Poisson's ratio, ν	0.3
	Density kg/m^3	2100
	Thickness,m	2.3
Sand and gravel	Young's modulus, MPa	50
	Poisson's ratio, ν	0.25
	Density kg/m^3	1800
	Thickness,m	3.0
Bridge (concrete)	Young's modulus, MPa	34500
	Poisson's ratio, ν	0.2
	Density kg/m^3	2500

Infinite elements were used at the boundaries of the embankment to overcome the problem of the stress waves generated from being reflected back into the model.

4.3 Initial verification of model

Table 3 compares the vibration levels and maximum accelerations measured in the field with those computed use the FE model for the rail, sleeper, at the bottom of the ballast, and at a depth of 2 m below the ballast bottom. All measurements were at a distance of 6 m from the abutment. From Table 3, although the computed values are slightly higher than those measured in the field, generally the results are in reasonable agreement. It is felt that the lower values determined from the field measurements may be as a results of high antecedent rainfall which occurred before the acceleration measurements were made, but after the field tests were carried out to determine the properties of the embankment.

Table 3 Comparison of field and model vibrations for transient zone components 6 m from the abutment

	Vibration level(dB)			Max acceleration(g)	
	Field	Computed	Difference (%)	Field	Computed
rail	153.7	155.0	0.8	23~50	40.00
sleeper	138.0	147.71	7.0	3~11	10.00
Subgrade at 0 m depth	102.5	109.6	6.9	0.3~0.8	1.0
Subgrade at 2m depth	100.5	105.0	4.5	0.4~0.6	0.40

Figure 13 shows the increase in vertical stress at different depths below the bottom of a sleeper obtained from the FE analysis as the train passes. Whilst measurement of stress were not undertaken in the field in this research project, the calculated stresses are in reasonable agreement with in situ measured values reported in the literature, albeit with different embankment properties. For example, [6] measured a vertical stress of approximately 85 kPa at a depth of 400mm below the sleeper on a heavy haul coal line in South Africa carrying trains with axle loads of 26 tonnes. This is in reasonable agreement to the one calculated by the model described herein of 89 kPa at a depth of 450mm.

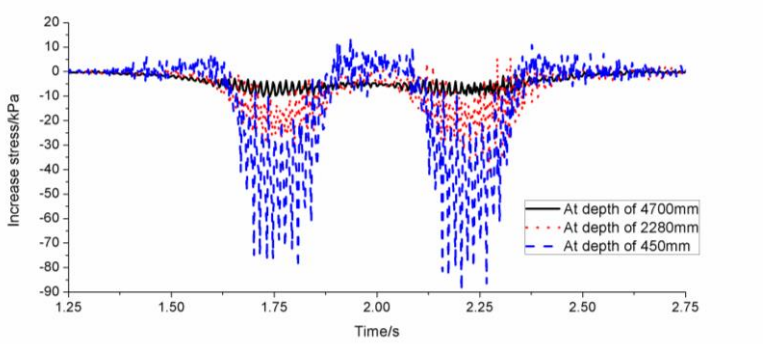

Fig.13 The increase in vertical stress at different depths below the bottom of a sleeper

4.4 Analysis

To better understand the implications of the proposed increases in train loads from 250 kN to 300 kN, measures of the safety, stability and train induced substructure damage were determined using the FE model and compared with design standards.

The first measure considered is the maximum vertical acceleration of the train which is a parameter used to ensure that the wagons run smoothly [15]. In Chinese railway standards an upper limit of 0.7g of the vertical acceleration of wagon is specified for heavy haul railways [15]. The maximum acceleration of wagon for wheel loads of 250 and 300 kN have been plotted in Figure 14. In addition accelerations of the train running from the abutment to the embankment and from the embankment to the bridge were compared. For the current axle loads, a maximum value of 0.154g well below that allowed in the Chinese code, is predicted for the train running from the less stiff embankment to the stiffer bridge structure. As expected this value is greater (for both wheel loads) than that for the train running from the bridge to the embankment, as in the former the wheel is lifted very quickly and large dynamic loads are applied to the rails. For the latter the track is subject to the larger dynamic loads [5]. It may be seen that the response of the wagon running on abutment (between 1.4 and 2.0s) is only slightly larger than its response on the subgrade.

Comment [b7]: Were these calculated using the existing wheel loads? If so is it possible to calculate using proposed axle loads and compare the two values?

Comment [b8]:

Comment [b9R8]: What does "smoothly" mean? Is it associated with safety, or damage to the wagon and or rail?

Comment [b10]: Is this subgrade to bridge or bridge to subgrade?

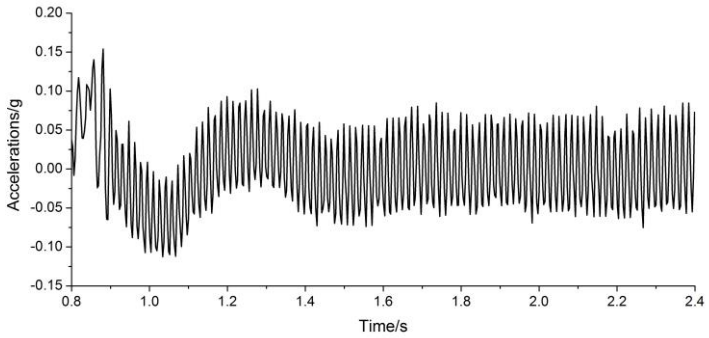

Figure 14 The accelerations at wagon at the train speed of 71km/h

The second measure considered is the wheel's contact force with the rail and is a parameter used to assess the likelihood of excess deterioration occurring at the wheel rail interface. Work by British Rail suggests that its maximum allowable value should be 250kN (or about twice the static wheel load) [16]. Using the FE model values of the wheel contact force were calculated for a train with axle loads of 250 and 300 kN travelling at 71 km/h. For an axle load of 250 kN, the contact force varies between 90 and 223 kN when considering the train running from the embankment to the bridge and of between x and y kN for the train running from the bridge to the embankment (see Figure 15). For the anticipated axle loads of 300 kN the calculated forces vary between x and y respectively for . Evidently the increase in axle load will result in values greater than the maximum value suggested by [] and may result in a significant increase in wear to both the wheel and rail. As expected the maximum contact forces are higher when, for the reasons discussed above, the train travels from the embankment to the bridge rather than vice versa.

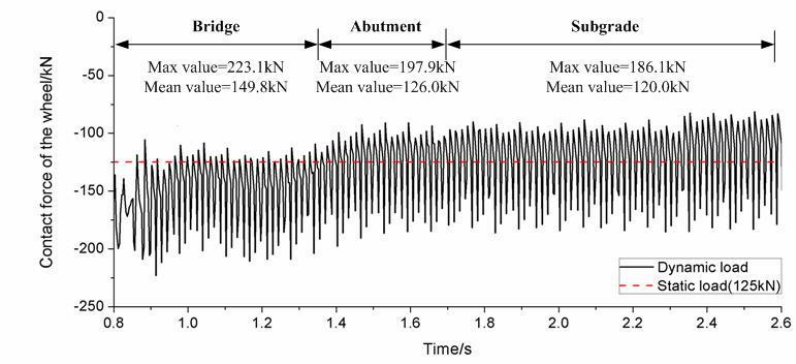

Figure 15: The contact force of wheel at the train speed of 71km/h

The third measure investigated is the axle load decrement ratio (PD) and is used to assess the likelihood of derailment. It is defined as follows:

$$PD = \frac{\Delta Q}{Q_s} = \frac{Q_s - Q}{Q_s} \qquad \text{(Equation 5)}$$

Comment [b11]: Equation number

Where, where Q_s and Q denote the static and dynamic wheel loads respectively.

Since the lateral stability of the wheel is a function of the vertical load acting on it, the higher the value of PD (and therefore the lower the dynamic load) the less the lateral stability of the wheelset.

An upper limit of 0.6 on the PD value was used in China's specifications for the design of railways [15], which will also be adopted herein. Figure 16 show the axle load decrement ratio at a speed of 71 km/h. It is found that the value of PD ranges from -0.5 to 0.49. the maximum value which occur on bridge is also smaller than the allowable value of 0.6 specified in the Chinese code. This indicated that the existing concrete T girder with running wagon of 250kN axle load has a higher possibility of derailment.

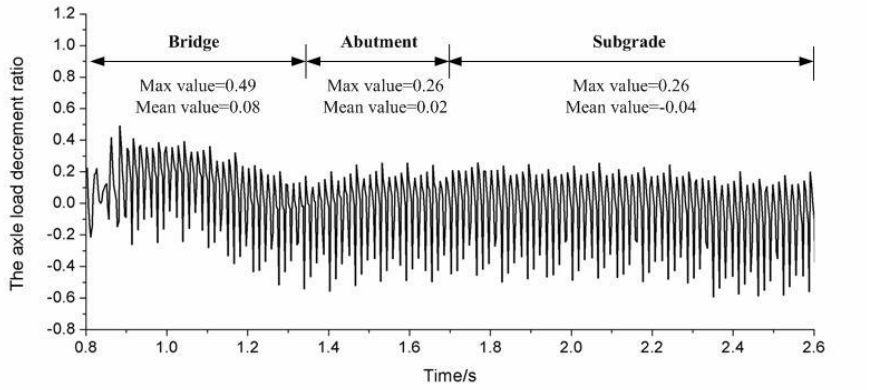

Fig.16 The axle load decrement ratio at the train speed of 71km/h

The last index adopted herein is the subgrade stress. A limit is placed on the maximum stress in order to minimize the subgrade deterioration. According to the existing specifications, the value of ballast and subgrade must not exceed 0.5MPa and 0.15MPa [15]. Fig 17 show increase stress of subgrade with relation to depth at the train speed of 71km/h. As can be seen, the stress in ballast and subgrade are well below the allowable stress. It may also be seen from Figure 17 that the maximum vertical stresses in the subgrade reduce rapidly with depth and that below approximately 3 m the increase in stress is hardly noticeable. For example, the stress reduces from 89kPa (at a depth of 0.45m) to 45kPa (at a depth of 2m) and 18 kPa to (at a depth of 4 m).This corroborates the findings of other authors [18~19] and suggests that the for modeling purposes only the upper 3 or 4 m need to be considered and that when designing the track structure particular attention should be given to the upper 3 m.

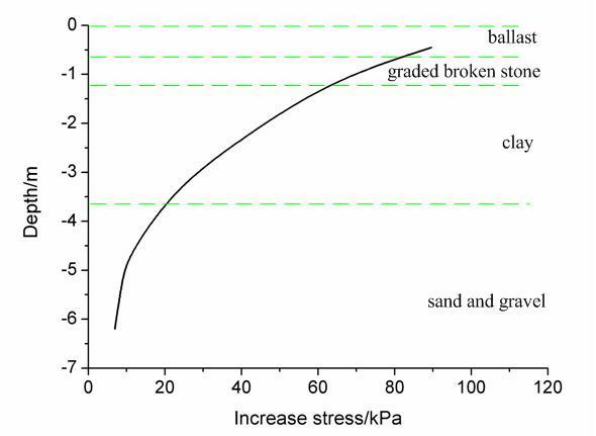

Fig.17 Increase stress of subgrade with relation to depth at the train speed of 71km/h

5 Concluding discussion

An extensive experiment was undertaken on a typical bridge-subgrade transition zone on the Shuohuang railway, China. This consisted of measuring accelerations and vibrations and the development of a moving wheel load 3D FE model. The following findings can be drawn from the numerical calculations and the field tests:

1. In the embankment a fundamental frequency of embankment acceleration occurs at 32Hz, which corresponds to the interval between sleepers. An additional harmonic at 64Hz can also be detected. Frequency peaks which relate to bogies and axles respectively are not apparent.

2. The vibrations from the excitation of the rail and sleepers are large within 6m from the abutment. This suggests that track will deteriorate more rapidly in the vicinity of the abutment and corroborates with in situ measurements of track geometry reported in the literature. For design purposes the findings show that to properly consider the effects of ground induced acceleration and vibration a moving load model should be used, particularly for railway track which will operate at high speeds or carry heavy load. Further it has been shown that in any such analysis it is important to consider axle configuration and that the four axles of a wagon may be considered to act as a single load pulse for the purposes of substructure structural design. Train induced stresses are concentrated in the upper 3 – 4m of the substructure and any design process should consider protecting existing materials adequately to this depth.

3. A dynamic three-dimensional finite element model was developed and validated using the measured accelerations. Results from the model suggest… safety, wear etc.. for 250 kN and for 300 kN

Initial results reported herein are promising although it is recognized that further verification and refinement of the model is both desired and necessary.

6 Acknowledgements

The work described in this paper has been supported by the National Natural Science Foundation of China (51008018) and the Research Fund for the Doctoral Program of Higher Education of China (20090009120020). The Birmingham Centre for Railway Research and Education at the University of Birmingham is also thanked for providing facilities to further the research.

References

1 **Zhai, W.M., Wang, K.Y., and Lin, J.H**. Modeling and experiment of railway ballast vibrations. *J. Sound Vibr,* 2004, 270(4), 673–683.

2 **Esveld, C.***Modern railway track*, 2nd edition, 2001 (MRT-Productions, Zaltbommel, TheNetherlands).

3 **Wu, T.X., and Thompson, D.J.The** vibration behavior of railway track at high frequencies under multiple preloads and wheel interactions. *Acoustical Society of America*,2000,108 (3),1046-1053

4 **Fryba,L.***Vibration of Solids and Structures under Moving Loads*. Thomas Telford, 3rd edition, 1999.

5 **Coelho, B., Hölscher, P., Priest, J., Powrie, W. and Barends, F.** An assessment of transition zone performance. *Proc. IMechE, Part F: J. Rail and Rapid Transit*, 2011, 225(2), 129-139.

6 **Priest,J.A.,Powrie,W.,Yang,L.,Grabe,P.J.,and Clayton,C.R.I.**Measurements of transient ground movements below a ballasted railway line.*Ge´otechnique* ,2010,60(9), 667–677.

7 **Yang,L.A., Powrie,W.,and Priest,J.A.** Dynamic stress analysis of a ballasted railway track bed during train passage. *Journal of Geotechnical and Geoenvironmental Engineering*, 2009, 135(5) ,680–689.

8 **Lei,X., and Zhang,B**.Influence of track stiffness distribution on vehicle and track interactions in track transition. *Proc. IMechE, Part F: J. Rail and Rapid Transit*, 2010, 224(1), 592–604.

9 **Gallego,Giner.I.,and López,Pita.A.**Numerical simulation of embankment–structure transition design. *Proc. IMechE, Part F: J. Rail and Rapid Transit*, 2009, 223(1), 331–343.

10 *IOtech Product Selection Guide*.Measurement Computing Corporation,2011.

11 **Grassie, S. L.** Models of railway track and vehicle–track interaction at high frequencies: Results of benchmark test. *Veh. Syst. Dyn.*, 1996, 25(supp): 243–262.

Comment [b12]: Please check date in references

12 **Xia H.** *Dynamic interactions between vehicles and structures.* Beijing: Science Press,2002.

13 **DONG Liang,ZHAO Cheng-gang.**Method fot dynamic response of subgrade subjectd to high-speed moving load. *Engineering Mechanics*, 2005, 25(11):231-240.

14 **Burrow,M.P.N.,and Chan,A.H.C**.Deflectometer-based analysis of ballasted railway tracks.*Geotechnical Engineering,* 2007, 160(GE3), 169–177.

15 **GB5599-85**. *Evaluation standard of dynamic characteristic of railway vehicle*. China planning press, 1985.

16 **Clark,R.A,Dean,P.A,Elkins,J.A,Newtons,S.G.**An investigation into the dynamic effects of railway vehicle running on corrugated rails.*Journal of Mechanical Engineering Science,*1982,24(2):65-76.

17 **Zienkiewicz,O.C., Chan,A.H.C., Pastor,M., Schefler,B.A. and Shiomi,T.** *Computational Geomechanics*. Wiley,Chichester, 1999

18 **Li,D. and Selig,E.T.** Resilient modulus for fine-grained. subgrade soils. *Journal of Geotechnical Engineering*, ASCE, 1994, 120(6), 939–957.

19 **Li, D. and Selig, E.T.** Method for railroad track foundation design. I: Development. *Journal of Geotechnical and Geoenvironmental Engineering, ASCE, 1998, 124(4).*

20 **ABAQUS Standard version 10.0.** Hibbitt, Karlsson and Sorensen, Inc., Pawtucket, RI, 2002.